Journal of Alloys and Compounds 480 (2009) 50–53

Contents lists available at ScienceDirect

Journal of Alloys and Compounds

journal homepage: www.elsevier.com/locate/jallcom

Optical anisotropy of near band-edge transitions in zinc oxide nanostructures

Ching-Hwa Ho[a,*], Jian-Shen Li[a], Yi-Jia Chen[a], Ching-Cherng Wu[a], Ying-Sheng Huang[b], Kwong-Kau Tiong[c]

[a] Department of Materials Science and Engineering, National Dong Hwa University, Shoufeng, Hualien 974, Taiwan
[b] Department of Electronic Engineering, National Taiwan University of Science and Technology, Taipei 106, Taiwan
[c] Department of Electrical Engineering, National Taiwan Ocean University Keelung 202, Taiwan

ARTICLE INFO

Article history:
Received 19 June 2008
Received in revised form 9 September 2008
Accepted 9 September 2008
Available online 21 November 2008

PACS:
78.20.−e
78.55.−m

Keywords:
Zinc oxide
Optical anisotropy

ABSTRACT

Optical anisotropy of the below and above band-edge transitions in three samples of well-aligned and tilted ZnO nanorods has been characterized using thermoreflectance (TR) and photoluminescence (PL) measurements in the temperature range between 30 and 300 K. The TR and PL spectra of the well-aligned nanorods with the largely top planes of $\{0001\}$ show considerable difference in energy with respect to those of the other tilted nanorods with the largely side planes of $\{10\bar{1}0\}$. Optical-axial anisotropy of the defects and band-edge excitonic transitions in the well-aligned and tilted ZnO nanorods are observed. Temperature dependences of transition energies of the defect emissions and band-edge excitons for the ZnO are analyzed. The crystallinity for the as-deposited ZnO thin films is also discussed.

1. Introduction

ZnO is a direct semiconductor that derives more interests for application in wide band-gap optoelectronics. Among them, the zinc oxide nanostructures received much attention for being room-temperature lasers, light-emitting diodes, transparent field-effect transistors, ultraviolet photodetectors, and solar cells. Especially, the ZnO nanorods gain increasing interest since they offer a unique opportunity for fabrication of nanoscale opto-electronic devices such as field-emission device [1], field-effect transistor [2], and light-emitting device [3]. Although various potential applications for the ZnO nanorods have been proposed, the experimental understanding on the optical anisotropy of the ZnO nanocrystal with different crystal axes is still rather incomplete.

In this paper, three samples of two well-aligned and one tilted ZnO nanorods have been characterized using TR and PL. Optical anisotropy of the defect and excitonic transitions in between the two different types of well-aligned and tilted nanorods is observed. The origins for the near band-edge transitions of the ZnO nanorods are evaluated and discussed.

2. Experiment

Three samples of ZnO nanorods were grown on Si and sapphire by metallorganic chemical-vapor deposition (MOCVD). Different setting of substrate temperature may result in lower growth rate and higher sintering rate, which can change the direction of ZnO nanorods from well-aligned vertical to tilted structures during the MOCVD growth [4]. Displayed in Fig. 1 are the field-emission scanning electron microscope (FESEM) images of the as-grown ZnO nanorods on different substrates of (a) sample A (ZnO/Si), (b) sample B (ZnO/sapphire), and (c) sample C (ZnO/sapphire), respectively. The diameters of the nanorods are estimated to be about 20–120 nm. For samples A and B, the ZnO were grown as the individual nanorods largely along the [0 0 0 1] direction, whereas most of the as-grown nanorods were closely contacted and even bended and merged demonstrated in sample C. X-ray diffraction measurements also showed that samples A and B have more strong (0 0 0 1) peak intensity than that of sample C. PL and TR were performed in two distinct spectral measurement systems. The experimental

---

* Corresponding author at: Department of Materials Science and Engineering, National Dong Hwa University, Shoufeng, Hualien 974, Taiwan. Fax: +886 38634200.
E-mail address: chho@mail.ndhu.edu.tw (C.-H. Ho).

0925-8388/$ – see front matter © 2008 Elsevier B.V. All rights reserved.
doi:10.1016/j.jallcom.2008.09.195

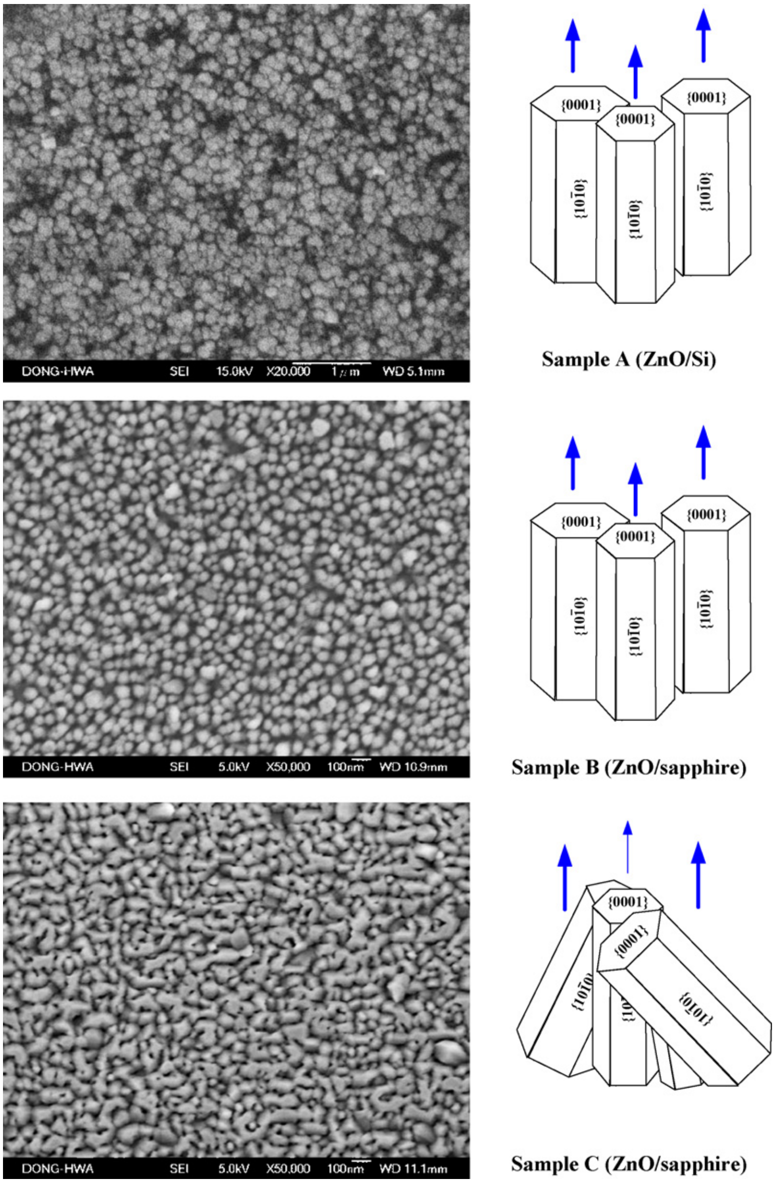

Fig. 1. The SEM images of three samples of two vertical-aligned and one tilted ZnO nanostructures. The light emissions from the surfaces of two different types of ZnO nanorods are also shown.

details of PL and TR measurements were described elsewhere [5]. Both measurements were done in the temperature range between 30 and 300 K.

3. Results and discussions

Temperature-dependent TR spectra of the well-aligned and tilted nanorods of (a) sample A, (b) sample B, and (c) sample C are shown in Fig. 2. The dashed lines are the experimental TR spectra and solid lines are the least-square fits to a first derivative Lorentzian line-shape function appropriate for the excitonic transitions [6]. The obtained transition energies of the band-edge free excitons (FXs) of A, B, and C indicate by arrows. As shown in the TR spectra of 30 K, the transition amplitudes for the FX series A–C in the well-aligned (samples A and B) and tilted (sample C) nanorods show different optical anisotropic behavior due to the geometric selection rule applied in different crystal planes of {0 0 0 1} or {1 0 $\bar{1}$ 0}. The optical-axial anisotropy is similar to that observed in the bulk ZnO crystal [7,8]. From Fig. 2, it is also found that all the excitonic transitions of FXs A_1, B_1, A_2, B_2, C_1, C_2, and C_∞ are clearly detected in the TR spectrum of sample C at 30 K while incomplete exciton series of A and B (missing A_1' and B_2') are observed in the TR spectrum of samples A and B. It also means that the binding energies and direct gaps for the A–C excitons in sample C can be analyzed from the Rydberg series using $E_n = E_\infty - R_y/n^2$. The values of binding energy R_y for the A–C excitons in sample C are determined to be 64, 60, and 61 meV. The threshold energies (i.e. E_∞) for the A–C excitons are determined to be 3.407, 3.421, and 3.481 eV at 30 K. As shown in Fig. 2(a), the TR spectra seem to contain two parts of contribution: one is coming from the A–C excitons, and the other is contributed by a broadened feature (~3.4 eV at 30 K). The broaden feature is coming from a E_0' transition in the silicon substrate. Also seeing from the TR spectra of 300 K in Fig. 2(a) and (b), for the well-aligned nanorods of sample A and sample B, the TR spectrum of sample B presents higher resolution and hence better crystallinity for the ZnO nanorods with respect to those shown in sample A. It is also evident from the SEM images of the well-aligned nanorods shown in Fig. 1, where sam-

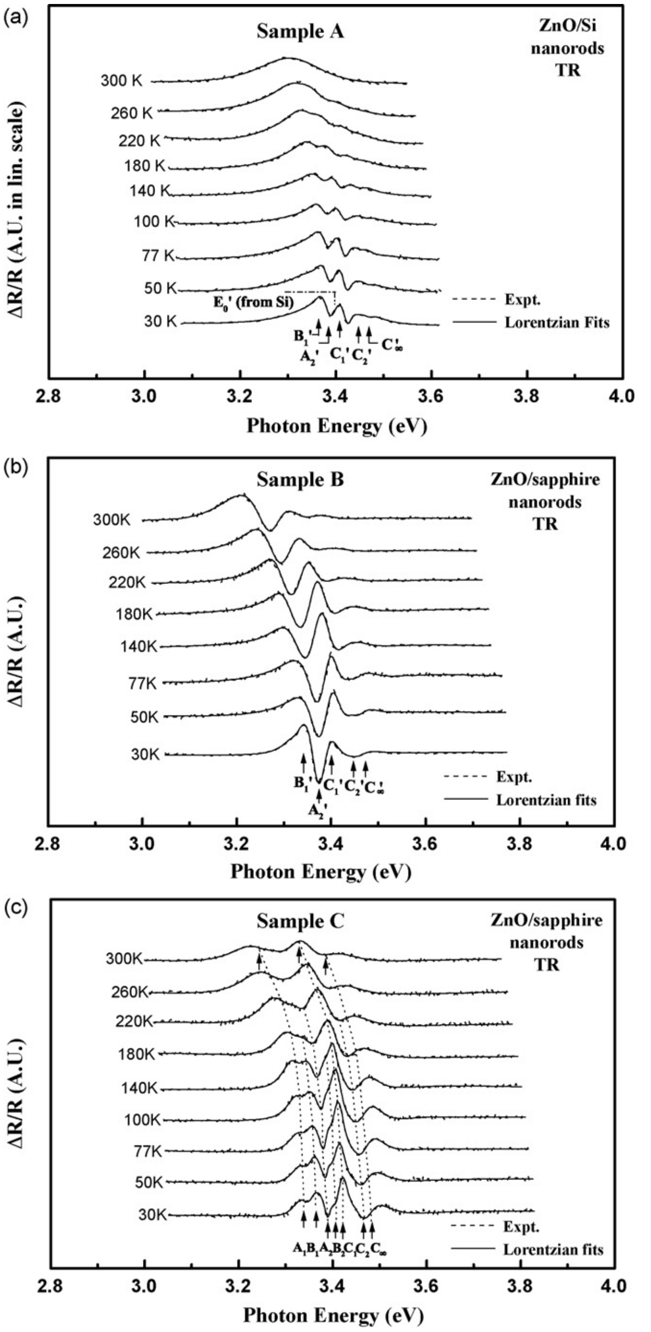

Fig. 2. Temperature-dependent TR spectra of (a) sample A, (b) sample B, and (c) sample C ZnO nanorods.

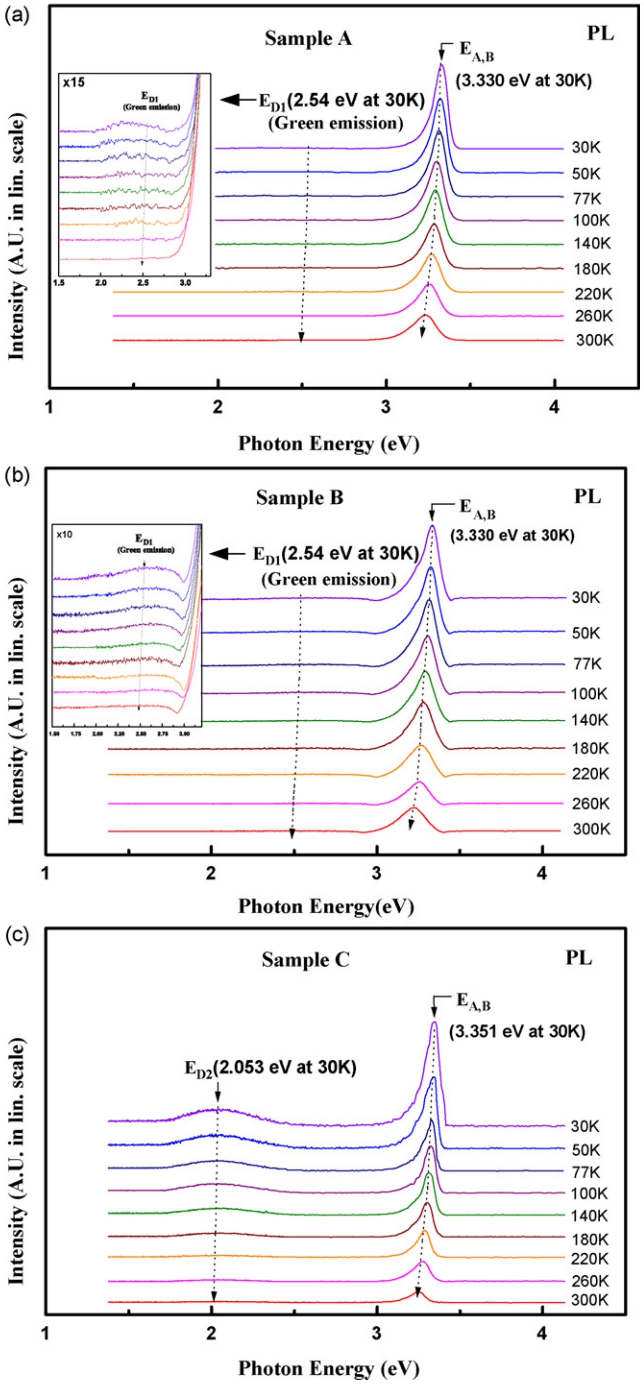

Fig. 3. Temperature-dependent PL spectra of the ZnO nanorods of (a) sample A, (b) sample B, and (c) sample C, respectively.

ple A shows more porous structures than the other samples of B and C.

As observing from the lineshape fits of Fig. 2, the energy value of each band-edge FX transition in the TR spectra reveals a blueshift of ∼20 meV detected from the well-aligned nanorods of samples A and B to the tilted nanostructures of sample C. The energy blueshift behavior is due to the surface effect. The mechanism accounting for the energy shift in ZnO nanostructures is the concentration of native defects on the surface area [9]. From the surface-to-volume ratios, it is inferred that the energy shift in all the excitonic transitions of the well-aligned and tilted nanorods is probably due to the influence of total surface area that available for the optical measurements. The energy values of the band-edge FX transitions in the TR spectrum of sample C at 30 K are higher than those of samples A and B due to the larger additional surface area of the lateral planes $\{1\,0\,\bar{1}\,0\}$ in sample C than those of the top planes $\{0\,0\,0\,1\}$ in samples A and B that were available for TR experiments.

Temperature-dependent PL spectra of the three ZnO nanorods are shown in Fig. 3. Two emission peaks of E_{D2} and $E_{A,B}$ are detected in the PL spectra of sample C at various temperatures while a weaker E_{D1} feature and one $E_{A,B}$ peak are observed in the samples of A and B due to different optical-axial anisotropy for the E_{D1} and E_{D2} defect emissions. The E_{D2} is the electronic recombination from the conduction band E_C to the interstitial level O_i which emits the PL

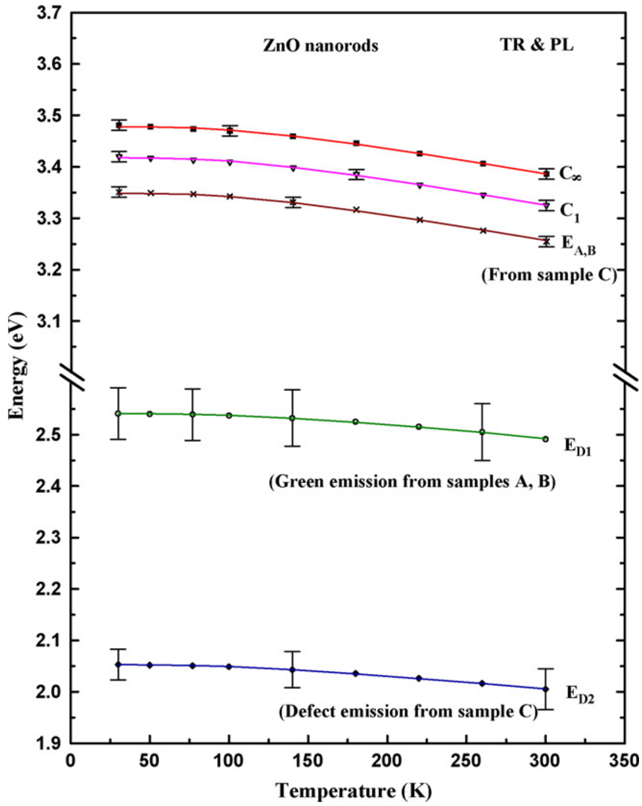

Fig. 4. Temperature dependences of transition energies of defects and excitonic transitions in the ZnO nanorods obtained by PL and TR experiments.

light from the lateral planes of the heaxagonal rods, where it is only observable when the ZnO nanorods are tilted to expose the side planes of $\{1\,0\,\bar{1}\,0\}$. The weak E_{D1} feature is the green luminescence, which is only detectable in the top plane of $\{0\,0\,0\,1\}$ in well-aligned ZnO nanorods seen from Fig. 3. The E_{D1} is induced by the antisite defect O_{Zn} or the oxygen vacancy in the zinc oxide. The $E_{A,B}$ feature at each temperature of the well-aligned nanorods is lower in energy (∼21 meV) with respect to the corresponding transition of the tilted structures due to the influence of total surface area that available for the optical measurement.

Temperature dependences of transition energies of band-edge free excitons and defect luminescences from TR and PL measurements are depicted in Fig. 4 with representative error bars. The solid lines are least-square fits to a Bose–Einstein relation expressed as $E_{iB}(T) = E_{iB}(0) - \varepsilon_B/[\exp(\hbar\omega_B/kT)) - 1]$. The obtained values of fitting parameters are $E_{iB}(0) = 3.478 \pm 0.005$, 3.404 ± 0.005, 3.350 ± 0.005, 2.052 ± 0.005, and 2.541 ± 0.005 eV for the features of C_∞, C_1, $E_{A,B}$, E_{D2} and E_{D1}, respectively. The obtained values of ε_B and $\hbar\omega_B$ are $\varepsilon_B = 200 \pm 25$ meV and $\hbar\omega_B = 30 \pm 2$ meV for C_∞, C_1 and $E_{A,B}$, and $\varepsilon_B = 100 \pm 25$ meV and $\hbar\omega_B = 30 \pm 2$ meV for E_{D2} and E_{D1}, respectively. The higher values of ε_B for C_∞, C_1 and $E_{A,B}$ indicate that the temperature-energy shift of the band-edge FXs $E_{A,B}$, C_1, and C_∞ is faster than that of the defect emissions of E_{D1} and E_{D2}. It shows the discrepancy of temperature energy shift in between a band-to-band and a defect transition.

4. Summary

Below and above band-edge transitions of the vertically aligned and tilted ZnO nanostructures have been characterized using PL and TR measurements in the temperature range between 30 and 300 K. The PL and TR spectra obviously show optical anisotropy in the defect transitions and band-edge free excitons of the well-aligned and tilted ZnO nanorods. The origins of the defect emissions of the ZnO nanorods are evaluated. E_{D1} is a green luminescence emitted largely from the top plane of $\{0\,0\,0\,1\}$. E_{D2} is also a defect luminescence caused by oxygen interstitials that inlaid in the lateral $\{1\,0\,\bar{1}\,0\}$ planes of the hexagonal rods. Temperature dependences of transition energies of the defect emissions and band-edge free excitons in the ZnO nanorods are analyzed. The result verifies the temperature-insensitive character of the defect emissions in the ZnO nanorods.

Acknowledgement

This work supported by the National Science Council of Taiwan under the grant No. NSC95-2221-E-259-031-MY3.

References

[1] R.C. Wang, C.P. Liu, J.L. Huang, S.J. Chen, Y.K. Tseng, S.C. Kung, Appl. Phys. Lett. 87 (2005) 013110.
[2] C. Xu, J. Chun, D.E. Kim, J.J. Kim, B. Chon, T. Joo, Appl. Phys. Lett. 90 (2007) 083113.
[3] Y.S. Chang, C.T. Chien, C.W. Chen, T.Y. Chu, H.H. Chiang, C.H. Ku, J.J. Wu, C.S. Lin, L.C. Chen, K.H. Chen, J. Appl. Phys. 101 (2007) 033502.
[4] C.H. Ho, Y.J. Chen, H.W. Jhou, J.H. Du, Opt. Lett. 32 (2007) 2765.
[5] C.H. Ho, H.W. Lee, Z.H. Cheng, Rev. Sci. Instrum. 75 (2004) 1098.
[6] D.E. Aspnes, in: M. Balkanski (Ed.), Handbook on Semiconductors, Amsterdam, North Holland, 1980.
[7] W.Y. Liang, A.D. Yoffe, Phys. Rev. Lett. 20 (1968) 59.
[8] J.E. Rowe, M. Cardona, F.H. Pollak, Solid State Commun. 6 (1968) 239.
[9] A.B. Djurišić, Y.H. Leung, Small 2 (2006) 944.